PAPER

NJC
www.rsc.org/njc

$[Cr^{III}(L)(CN)_4]^-$: a new building block in designing cyanide-bridged 4,2-ribbon-like chains $\{[Cr^{III}(L)(CN)_4]_2Mn(H_2O)_2\}\cdot nH_2O$ [L = 2-aminomethylpyridine (n = 6) and 1,10-phenanthroline (n = 4)]†

Luminita Toma,[a] Rodrigue Lescouëzec,[a] Jacqueline Vaissermann,[b] Patrick Herson,[b] Valérie Marvaud,[b] Francesc Lloret[a] and Miguel Julve*[a]

[a] *Departament de Química Inorgànica, Instituto de Ciencia Molecular, Facultat de Química de la Universitat de Valencia, Avda. Dr. Moliner 50, 46100 Burjassot, Valencia, Spain. E-mail: miguel.julve@uv.es*

[b] *Laboratoire de Chimie Inorganique et Matériaux Moléculaire (CNRS UMR 7071), Université Pierre et Marie Curie, 75252 Paris cedex 05, France*

Received (in Montpellier, France) 1st September 2004, Accepted 3rd November 2004
First published as an Advance Article on the web 16th December 2004

The preparation, X-ray crystallography and magnetic study of compounds $PPh_4[Cr(ampy)(CN)_4]\cdot H_2O$ (**1**), $PPh_4[Cr(phen)(CN)_4]\cdot H_2O\cdot CH_3OH$ (**2**), $\{[Cr(ampy)(CN)_4]_2Mn(H_2O)_2\}\cdot 6H_2O$ (**3**) and $\{[Cr(phen)(CN)_4]_2Mn(H_2O)_2\}\cdot 4H_2O$ (**4**), with PPh_4^+ = tetraphenylphosphonium cation, ampy = 2-aminomethylpyridine and phen = 1,10-phenanthroline, are reported here. **1** and **2** are mononuclear complexes whereas **3** and **4** are 4,2-ribbon-like bimetallic chains. The magnetic properties of **1**–**4** were investigated in the temperature range 1.9–300 K. A quasi Curie law behaviour for a magnetically isolated spin quartet is observed for **1** and **2**. Compounds **3** and **4** are ferrimagnetic $Cr^{III}_2Mn^{II}$ chains, which exhibit a metamagnetic behaviour, the values of the critical field being H_c = 1 T (**3**) and 5000 G (**4**), which is due to the occurrence of weak interchain antiferromagnetic interactions. Below *ca.* 4.0 K, compound **4** shows a spin-canted structure with a narrow hysteresis loop, the value of the coercive field being 50 G.

Introduction

Extended metal-cyanide frameworks have been subject of intensive research during the last decade.[1,2] The variety in their structures associated with their interesting functional properties, such as molecular sieves,[3] hosts for small molecules and ions,[1,4] catalysts for the production of ether polyols or polycarbonates,[5] room temperature magnets,[6–8] electrochemically tunable magnets,[9] photo-magnetic materials[9a,10] and magneto-optical effects,[11] make them suitable compounds for the design of new materials. In general, this vast chemistry deals with the highly insoluble three-dimensional Prussian-Blue analogues, which are obtained by reacting the hexacyanometallate unit $[M(CN)_6]^{(6-m)-}$ with the fully solvated species $[M'(H_2O)_6]^{m'+}$ (where M and M′ are paramagnetic metal ions and m and m' are the charges of M and M′ respectively). In an attempt to extend this chemistry into the molecular regime, several research groups have developed an alternative synthetic route, which consists in using stable cyanide-bearing six-coordinate complexes of general formula $[M(L)(CN)_x]^{(x+1-3)-}$ with M = trivalent transition metal ion, where the overall charge and the number of cyanide ligands are dependent on the denticity and charge (l) of the polydentate L ligand.[5,12–18] For the sake of brevity, we will illustrate the richness of this strategy with three illustrative examples. The first two concern the case where L is a tridentate ligand such as 1,4,7-trimethyltriazacyclonane (Me_3tacn) or bis(2-pyridylcarbonyl)amidate anion (bpca). The resulting mononuclear tricyano complexes of formula $[Cr(Me_3tacn)(CN)_3]$ and $[Fe(bpca)(CN)_3]^-$ exhibit *fac* and *mer* arrangements of the cyanide ligands, respectively. Their use as ligands towards metal ions affords cage compounds possessing a cubic arrangement of eight chromium atoms linked through edge-spanning cyanide bridges[12b] and ladder-like chains with a single cyanide bridge in each rung and rod.[14g] These two topologies (boxes and ladder-like chains) are the consequence of a stereochemical control, which is exerted by the *fac* and *mer* arrangements of the cyanide ligands in the respective building blocks. The last example deals with the design of 4,2-ribbon-like bimetallic chains[19] by using the $[FeL(CN)_4]^-$ unit [L = 1,10-phenanthroline (phen) or 2,2′-bipyridine (bipy)] as a ligand towards fully solvated metal ions.[14a,e,f] Some of them exhibit slow magnetic relaxation and hysteresis effects, being thus among the scarce examples of single-chain magnets (SCM).[14e,f,20] We report here on two new cyanide-bearing chromium(III) building blocks of formula $PPh_4[Cr(ampy)(CN)_4]\cdot H_2O$ (**1**) and $PPh_4[Cr(phen)(CN)_4]\cdot H_2O\cdot CH_3OH$ (**2**), with PPh_4^+ = tetraphenylphosphonium cation, ampy = 2-aminomethylpyridine and phen = 1,10-phenanthroline, and their respective 4,2-ribbon-like bimetallic chains $\{[Cr(ampy)(CN)_4]_2Mn(H_2O)_2\}\cdot 6H_2O$ (**3**) and $\{[Cr(phen)(CN)_4]_2Mn(H_2O)_2\}\cdot 4H_2O$ (**4**), which are obtained by using **1** and **2** as complex ligands toward fully hydrated manganese(II) ions. The preparation of **1**–**4** and their magnetostructural investigation are presented hereunder.

† Electronic supplementary information (ESI) available: translational quadruple phenyl embrace (TQPE), $\chi_M T$ versus T plot and structure view in the *bc* plane for **1**; parallel quadruple phenyl embrace (PQPE) and structure view in the *bc* plane for **2**; hysteresis loop of **4** at 2.0 K. See http://www.rsc.org/suppdata/nj/b4/b413473g/

DOI: 10.1039/b413473g

Experimental

Materials

Chromium(III) chloride hexahydrate, manganese(II) nitrate tetrahydrate, 2-aminomethylpyridine, 1,10-phenanthroline, potassium cyanide, tetraphenylphosphonium chloride and lithium perchlorate trihydrate were purchased from commercial sources and used as received. $[Cr_2(CH_3COO)_4(H_2O)_2]$ was prepared according to the literature[21] and was kept in a dessicator over calcium chloride and under anaerobic conditions. Distilled water, methanol and acetonitrile of analytical grade quality were used as solvents. Elemental analyses (C, H, N) were performed at the Microanalytical Service of the Universidad Autónoma de Madrid. Cr : P (**1** and **2**) and Cr : Mn (**3** and **4**) molar ratios of 1 : 1 and 2 : 1, respectively, were determined by electron probe X-ray microanalysis at the Servicio Interdepartamental of the University of Valencia.

Preparations

$PPh_4[Cr(ampy)(CN)_4]\cdot H_2O$ (1) and $PPh_4[Cr(phen)(CN)_4]\cdot H_2O\cdot CH_3OH$ (2). Compounds **1** and **2** were prepared by the same synthetic procedure, the only difference being in the nature of the organic ligand. In a typical experiment, concentrated hydrochloric acid (3.34 cm^3, 20 mmol) was added to a dioxygen-free aqueous suspension (20 cm^3) of freshly prepared chromium(II) acetate (1.88 g, 5 mmol) with continuous stirring and under argon atmosphere. The resulting blue solution became brown when mixed with 2-aminomethylpyridine (1.08 g, 10 mmol). Then, the solution was stirred for 10 min. Potassium cyanide (2.60 g, 40 mmol), dissolved in a minimum amount of dioxygen-free hot water (10 cm^3), was added. A brown solid separated and was collected by filtration in the open air while the mother liquor was poured into a concentrated aqueous solution containing PPh_4Cl (3.75 g, 10 mmol). The solution turned yellow and a crop of a yellow solid precipitated after standing at room temperature for several minutes. Crude **1** was collected by filtration, washed with small portions of cold water and purified by recrystallisation in acetonitrile. X-Ray quality crystals were grown by slow evaporation of this recrystallised product in $H_2O : CH_3CN$ (1 : 20, v/v) mixture and isolated as well-shaped yellow parallelepipeds. The yield was ~35%. IR (KBr pellets): ν(CN stretching) = 2129s cm^{-1}; anal. calcd for $C_{34}H_{30}CrN_6OP$: C, 65.69; H, 4.83; N, 13.52; found: C, 67.91; H, 4.68; N, 14.79%.

For **2**, 1,10-phenanthroline (1.98 g, 10 mmol) was used; recrystallisation in $H_2O : CH_3OH$ (1 : 20, v/v) mixture; yellow parallelepipeds; yield ~35%. IR (KBr pellets): ν(CN stretching) = 2133w, ν(OH) = 3676s cm^{-1} (CH_3OH solvent molecule); anal. calcd for $C_{41}H_{34}CrN_6O_2P$: C, 67.85; H, 4.68; N, 11.58; found: C, 68.46; H, 5.09; N, 12.24%.

$\{[Cr(ampy)(CN)_4]_2Mn(H_2O)_4\}\cdot 6H_2O$ (3) and $\{[Cr(phen)(CN)_4]_2Mn(H_2O)_4\}\cdot 4H_2O$ (4). In a typical experiment, an aqueous solution (10 cm^3) of lithium (2-aminomethylpyridine)(tetracyano)chromate(III) dihydrate‡ (0.061 g, 0.2 mmol) was poured into an aqueous solution (10 cm^3) of $Mn(NO_3)_2\cdot 4H_2O$ (0.025 g, 0.1 mmol). Yellow plates of **3** were grown from the resulting yellow solution by slow evaporation at room temperature. The yield was almost quantitative. IR (KBr pellets): ν(CN stretching) = 2167s, 2130 and 2139m cm^{-1}; anal. calcd for $C_{20}H_{32}Cr_2MnN_{12}O_8$: C, 33.02; H, 4.40; N, 23.10; found: C, 34.67; H, 3.15; N, 21.33%.

For **4**, lithium (1.10-phenanthroline)(tetracyano)chromate(III) dihydrate‡ (0.069 g, 0.2 mmol) was used; yellow parallelepipeds; yield almost quantitative. IR (KBr pellets): ν(CN stretching) = 2164m, 2153, 2143 cm^{-1}; anal. calcd for $C_{32}H_{28}Cr_2MnN_{12}O_6$: C, 46.00; H, 3.35; N, 20.11; found: C, 47.91; H, 2.94; N, 22.14%.

Physical characterisation

Infrared spectra (KBr pellets) were obtained on a Nicolet Avatar 320 FT-IR spectrophotometer. Magnetic susceptibility measurements on polycrystalline samples of **1**–**4** were carried out with a Quantum Design SQUID magnetometer in the temperature range 1.9–290 K and under applied magnetic fields ranging from 50 G to 1 T. Magnetisation *versus* magnetic field measurements of **1**–**4** were carried out at 2.0 K in the field range 0–5 T. Alternating current magnetic susceptibility measurements on **3** and **4** were performed at low temperatures ($T < 15$ K) in the frequency range 0.1–1400 Hz and under an oscillating magnetic field of 1 G. Diamagnetic corrections of the constituent atoms were estimated from Pascal constants[22] as -379×10^{-6} (**1**), -460×10^{-6} (**2**), -409×10^{-6} (**3**) and -500×10^{-6} (**4**) $cm^3\ mol^{-1}$.

X-Ray analysis and structure refinement

Crystals of dimensions 0.20 × 0.30 × 0.60 (**1**), 0.20 × 0.20 × 0.30 (**2** and **3**) and 0.20 × 0.30 × 0.30 (**4**) mm^3 were mounted on Enraf-Nonius MACH3 (**1** and **2**) and CAD4 (**3** and **4**) diffractometers and used for data collection. Diffraction data for **1**–**4** were collected at room temperature by using graphite-monochromated MoKα radiation (λ = 0.71073 Å) with the $\omega-2\theta$ method. Accurate cell dimensions and orientation matrices were obtained by least-squares refinements of 25 accurately centred reflections with $13 < \theta < 14^\circ$ (**1**–**4**). No significant variations were observed in the intensities of two checked reflections (**1**–**3**) during data collection; for **4**, a decay of 58% was observed and the data were accordingly scaled. The data were corrected for Lorentz and polarisation effects (**1**–**4**). Absorption corrections on **1**–**4** were applied using DIFABS[23] (**1**, **2** and **4**) and the φ-scan curve (**3**). A summary of crystallographic data and structure refinement is given in Table 1.§

The structures of **1**–**4** were solved by direct methods through the SHELX-86[24] program and subsequently completed by Fourier recycling on *F*. The final full-matrix least-squares refinement for **1**–**4** was done by the PC version of CRYSTALS[25] and the function minimised was $\sum w(|F_o| - |F_c|)^2$ where $w = w'[1-(||F_o|-|F_c||)/6\sigma(F_o)^2]^2$, w' being equal to $1/\sum_\rho A_r T_r(X)$ with three coefficients for a Chebyshev series [11.7, −2.02 and 9.96 (**1**), 5.48, −0.791 and 4.17 (**2**) 22.6, −7.99 and 16.0 (**3**) and 7.59, −0.908 and 4.89 (**4**)], for which $X = F_c/F_c(\max)$. All non-hydrogen atoms in **1**–**4** were refined anisotropically. The hydrogen atoms of the ampy ligand (with the exception of those of the amino group that were neither located nor introduced) for **1** and **3** and the phen ligand for **2** and **4**, together with those of tetraphenylphosphonium (**1** and **3**), were introduced in calculated positions. The hydrogen atoms of the coordinated water molecules in **2** were located by means of a difference Fourier map, whereas those of the methanol molecule (**2**) as well as crystallisation (**1**–**4**) and coordination (**4**) water molecules were neither located nor introduced. The coordinates of the hydrogen atoms were not refined, but they were allocated an overall isotropic thermal parameter. The final geometrical calculations and graphical manipulations for **1**–**4** were carried out with the PARST[26] and CRYSTALMAKER[27] programs.

‡ These products were obtained as yellow solids by a metathesis reaction of stoichiometric amounts of lithium perchlorate and **1** and **2**, respectively, in acetonitrile

§ CCDC reference numbers 245541 (**1**), 245542 (**2**), 245543 (**3**) and 245544 (**4**). See http://www.rsc.org/suppdata/nj/b4/b413473g/ for crystallographic data in .cif or other electronic format.

Table 1 Summary of crystallographic data and structure refinement for $PPh_4[Cr(ampy)(CN)_4]\cdot H_2O$ (**1**), $PPh_4[Cr(phen)(CN)_4]\cdot H_2O\cdot CH_3OH$ (**2**), $[\{Cr(ampy)(CN)_4\}_2Mn(H_2O)_2]\cdot 6H_2O$ (**3**) and $[\{Cr(phen)(CN)_4\}_2Mn(H_2O)_2]\cdot 4H_2O$ (**4**)

Compound	1	2	3	4
Chemical formula	$C_{34}H_{30}CrN_6OP$	$C_{41}H_{34}CrN_6O_2P$	$C_{20}H_{32}Cr_2MnN_{12}O_8$	$C_{32}H_{28}Cr_2MnN_{12}O_6$
FW/g mol^{-1}	621.62	725.73	727.47	835.58
Crystal system	Triclinic	Monoclinic	Triclinic	Monoclinic
Space group	$P(-1)$	$P2_1/c$	$P(-1)$	$P2_1/n$
a/Å	8.723(7)	9.369(3)	7.191(5)	7.641(5)
b/Å	13.581(2)	27.635(7)	10.566(7)	15.569(4)
c/Å	13.656(3)	14.477(4)	11.906(5)	15.490(4)
α/°	94.42(1)	90	101.66(4)	90
β/°	93.37(5)	97.52(2)	107.08(4)	93.69(4)
γ/°	92.69(4)	90	96.72(5)	90
U/Å^3	1608(1)	3716(2)	831.7(9)	1839(1)
Z	2	4	1	2
T/K	295	295	295	295
μ(MoKα)/cm^{-1}	4.41	3.49	10.72	9.78
Reflections collected	8232	7116	3182	3630
Independent reflections	7731	6521	2925	3612
Observed reflections[a]	4483	3210	2668	2700
R_{int}	0.02	0.05	0.03	0.03
R (all data)	0.1079	0.1208	0.0630	0.1139
R_w (all data)	0.0757	0.0594	0.0632	0.0891
R^a	0.053	0.047	0.060	0.091
$R_w{}^{ab}$	0.059	0.055	0.062	0.081

[a] $I > 3\sigma(I)$. [b] $R = [\Sigma(|F_o| - |F_c|)/\Sigma|F_o|]^{1/2}$ and $R_w = [\Sigma w(|F_o|^2 - |F_c|^2)/\Sigma w|F_o|^2]^{1/2}$.

Results and discussion

Description of the structures

$PPh_4[Cr(ampy)(CN)_4]\cdot H_2O$ (1). The crystallographic analysis of **1** (Table 2) shows that its structure consists of mononuclear $[Cr(ampy)(CN)_4]^-$ anions (Fig. 1), tetraphenylphosphonium cations and uncoordinated water molecules. Hydrogen bonds involve the crystallisation water molecule and one cyanide nitrogen atom [N(2)] from the $[Cr(ampy)(CN)_4]^-$ unit [2.919(4) Å for N(2)···O(1a); (a) = $2-x$, $1-y$, $1-z$]. Each chromium atom is six-coordinated with two ampy nitrogen atoms and four cyanide carbon atoms in a distorted octahedral geometry. The small bite angle of the chelating ampy [79.21(1)° for N(11)–Cr(1)–N(12)] is the main factor accounting for this distortion from the ideal geometry. The values of the Cr–N(ampy) bond lengths [2.082(2) and 2.088(2) Å for Cr(1)–N(12) and Cr(1)–N(11), respectively] and the Cr–C(cyano) bond lengths [2.058(3)–2.077(3) Å] agree with values recently reported for the tetraphenylphosphonium 2,2′-bipyridine(tetracyano)chromate(III) complex.[28] The Cr(1)–C–N angles for the terminally bound cyanide ligands in **1** are quasi-linear [176.9(3)–178.6(3)°]. The values of the cyanide C–N bonds vary in the range 1.146(4)–1.138(4) Å. The N(12), C(11), C(12), C(13), C(14), C(15) and C(16) atoms of the ampy ligand are coplanar [N(11) and Cr(1) are localised at 0.57 and 0.10 Å, respectively, from this mean plane]. No significant π–π staking interactions between adjacent ampy ligands are observed. The bulky tetraphenylphosphonium cation exhibits the expected tetrahedral shape and its bond lengths and angles are as expected. Interestingly, the PPh_4^+ cations are grouped by pairs along the b axis, the resulting motif being the translational quadruple phenyl embrace, TQPE,[29] with a P···P separation of 6.970(1) Å (see the electronic supplementary information).

Regular alternating of two kind of layers growing in the bc plane {hydrophobic cationic (tetraphenylphosphonium) and

Table 2 Selected bond distances (Å) and angles (°) in complex **1**[a]

Cr(1)–N(11)	2.088(2)	Cr(1)–N(12)	2.082(2)
Cr(1)–C(1)	2.058(3)	Cr(1)–C(2)	2.058(3)
Cr(1)–C(3)	2.077(3)	Cr(1)–C(4)	2.077(3)
C(1)–N(1)	1.146(4)	C(2)–N(2)	1.139(4)
C(3)–N(3)	1.139(4)	C(4)–N(4)	1.138(4)
N(11)–Cr(1)–N(12)	79.21(10)	N(11)–Cr(1)–C(1)	172.88(10)
N(11)–Cr(1)–C(2)	95.61(11)	N(11)–Cr(1)–C(3)	89.83(11)
N(11)–Cr(1)–C(4)	90.89(11)	N(12)–Cr(1)–C(1)	93.84(10)
N(12)–Cr(1)–C(2)	174.33(11)	N(12)–Cr(1)–C(3)	92.41(11)
N(12)–Cr(1)–C(4)	89.64(11)	C(1)–Cr(1)–C(2)	91.40(11)
C(1)–Cr(1)–C(3)	88.92(11)	C(1)–Cr(1)–C(4)	90.59(11)
C(2)–Cr(1)–C(3)	89.86(12)	C(2)–Cr(1)–C(4)	88.13(12)
C(3)–Cr(1)–C(4)	177.92(12)	Cr(1)–C(1)–N(1)	178.2(3)
Cr(1)–C(2)–N(2)	176.9(3)	Cr(1)–C(3)–N(3)	177.7(3)
Cr(1)–C(4)–N(4)	178.6(3)		

Hydrogen bonds[bc]	A	D	A···D
	O(1a)	N(2)	2.919(4)

[a] Estimated standard deviations in the last significant digits are given in parentheses. [b] A = acceptor, D = donor. [c] Symmetry code: (a) = $2-x$, $1-y$, $1-z$.

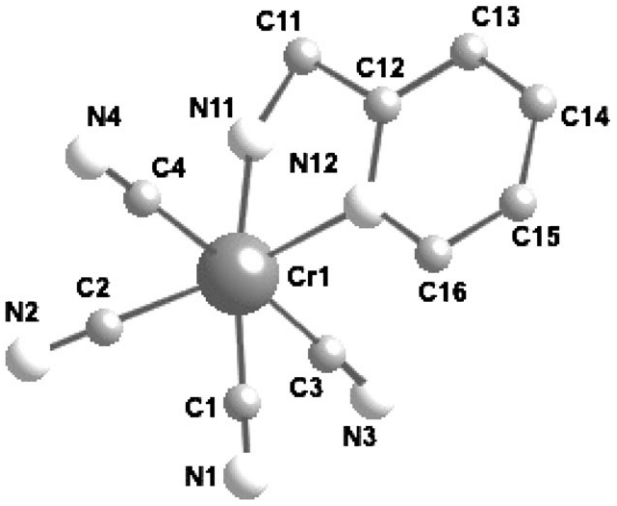

Fig. 1 Perspective drawing of the $[Cr(ampy)(CN)_4]^-$ anion of complex **1** with atom numbering shown. Hydrogen atoms from the ampy ligand have been omitted for the sake of clarity.

Table 3 Selected bond distances (Å) and angles (°) in complex **2**[a]

Cr(1)–N(11)	2.086(3)	Cr(1)–N(12)	2.087(3)
Cr(1)–C(1)	2.045(4)	Cr(1)–C(2)	2.059(5)
Cr(1)–C(3)	2.058(5)	Cr(1)–C(4)	2.074(5)
C(1)–N(1)	1.134(6)	C(2)–N(2)	1.142(5)
C(3)–N(3)	1.133(6)	C(4)–N(4)	1.132(6)
N(11)–Cr(1)–N(12)	79.15(13)	N(11)–Cr(1)–C(1)	171.58(16)
N(11)–Cr(1)–C(2)	94.95(15)	N(11)–Cr(1)–C(3)	92.05(16)
N(11)–Cr(1)–C(4)	90.05(15)	N(12)–Cr(1)–C(1)	92.71(15)
N(12)–Cr(1)–C(2)	174.03(15)	N(12)–Cr(1)–C(3)	91.33(15)
N(12)–Cr(1)–C(4)	91.74(15)	C(1)–Cr(1)–C(2)	93.14(17)
C(1)–Cr(1)–C(3)	90.30(19)	C(1)–Cr(1)–C(4)	88.02(18)
C(2)–Cr(1)–C(3)	89.83(18)	C(2)–Cr(1)–C(4)	87.28(18)
C(3)–Cr(1)–C(4)	176.56(18)	Cr(1)–C(1)–N(1)	176.6(4)
Cr(1)–C(2)–N(2)	177.8(4)	Cr(1)–C(3)–N(3)	178.7(5)
Cr(1)–C(4)–N(4)	175.1(4)		

Hydrogen bonds[bc]	A	D	A···D
	O(11a)	N(2)	2.881(6)
	O(11b)	N(4)	2.816(6)
	O(10)	O(11)	2.669(6)

[a] Estimated standard deviations in the last significant digits are given in parentheses. [b] A = acceptor, D = donor. [c] Symmetry code: (a) = x, $3/2-y$, $1/2+z$, (b) = $-x$, $-1/2+y$, $1/2-z$.

hydrophilic anionic [Cr(ampy)$(CN)_4$]$^-$} occurs in the unit cell (see Fig. S1 in the ESI). The value of the shortest intermolecular chromium–chromium separation is 6.326(1) Å [Cr(1)···Cr(1b); (b) = $1-x$, $-y$, $2-z$].

PPh_4[Cr(phen)$(CN)_4$]·CH_3OH·H_2O (2). The crystallographic analysis of **2** (Table 3) shows that its structure consists of mononuclear [Cr(phen)$(CN)_4$]$^-$ anions (Fig. 2), tetraphenylphosphonium cations and uncoordinated water and methanol molecules. The crystallisation water molecule is involved in hydrogen bonding with two of the cyanide nitrogen atoms of the anionic unit [2.816(6) and 2.881(6) Å for N(4)···O(11a) and N(2)···O(11b), respectively; (a) = x, $3/2-y$, $1/2+z$ and (b) = $-x$, $-1/2+y$, $1/2-z$] and the oxygen atom of the methanol molecule [2.669(6) Å for O(11)···O(10)]. Each chromium atom is six-coordinate with two phen nitrogen atoms and four cyanide carbon atoms in a distorted octahedral geometry. The small bite angle of the chelating phen [79.15(13)° for N(11)–Cr(1)–N(12)] is the main factor accounting for this distortion from the ideal geometry. The values of Cr–N(phen) bond lengths [2.086(3) and 2.087(3) Å for Cr(1)–N(11) and Cr(1)–N(12)] and the Cr–C(cyano) bond lengths [2.045(4)–2.074(5) Å] agree with those reported for compound **1** and the tetraphenylphosphonium 2,2′-bipyridine(tetracyano)

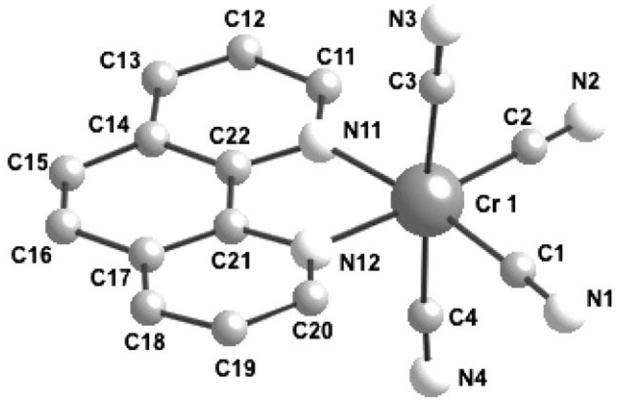

Fig. 2 Perspective drawing of the [Cr(phen)$(CN)_4$]$^-$ anion of complex **2** showing the atom numbering. Hydrogen atoms from the phen ligand have been omitted for the sake of clarity.

chromate(III) complex.[28] The Cr(1)–C–N angles for the terminally bound cyanide ligands in **2** are quasi-linear [175.1(4)–178.7(5)°]. The values of the cyanide C–N bonds vary in the range 1.142(4)–1.132(6) Å. Bond distances and angles within this ligand are in agreement with those reported for free phen.[30] Although the shortest intermolecular phen–phen contact is *ca.* 3.48 Å, the large slipping of the phen planes precludes any significant π–π interaction. Interestingly, the PPh_4^+ cations are grouped by pairs along the *b* axis, the resulting motif being the parallel quadruple phenyl embrace, PQPE,[29] with a P···P separation of 7.397 Å (see Fig. S3 in the ESI). Regular alternating of two types of layers growing in the *bc* plane {hydrophobic cationic (tetraphenylphosphonium) and hydrophilic anionic [Cr(phen)$(CN)_4$]$^-$} occurs in the unit cell (see Fig. S4 in the ESI). The value of the shortest intermolecular chromium–chromium separation is 8.094(1) Å [Cr(1)···Cr(1d); (d) = $1-x$, $1-y$, $1-z$].

[Cr(ampy)$(CN)_4]_2Mn(H_2O)_4\cdot 6H_2O$ (3) and [Cr(phen)$(CN)_4]_2Mn(H_2O)_4\cdot 4H_2O$ (4). The structures of **3** and **4** consist of neutral cyanide-bridged crossed Cr(III)–Mn(II) zigzag chains of general formula [Cr(L)$(CN)_4]_2Mn(H_2O)_4$, with L = ampy (**1**) and phen (**2**), which are linked by hydrogen bonds and van der Waals forces. Within each chain, the [Cr(L)$(CN)_4$]$^-$ unit acts as a bismonodentate bridging ligand towards two *trans*-diaquamanganese(II) entities through two of its four cyanide groups in *cis* positions, affording bimetallic chains, which run parallel to the *a* axis [Fig. 3 (**3**) and Fig. 4 (**4**)]. This structural type has been described as a 4,2-ribbon-like chain[19] and it is isostructural with the bimetallic one-dimensional compounds {[Fe^{III}(L)$(CN)_4]_2M^{II}(H_2O)_2$}·$4H_2O$ (L = phen; M = Co, Mn and Zn, and L = bipy; M = Co)[14a,e] and {[Cr^{III}(bipy)$(CN)_4]_2Mn^{II}(H_2O)_2$}·$4H_2O$.[28]

Each coordinated water molecule in **3** (Table 4) is hydrogen-bonded to two crystallisation water molecules [2.646(7) and 2.738(5) Å for O(1)···O(12c) and O(1)···O(13d), respectively; (c) = $1+x$, $-1+y$, z and (d) = x, $-1+y$, z]. One of these uncoordinated water molecules is linked to the remaining crystallisation water [2.741(9) Å for O(11)···O(12)], whereas the other one is linked to the terminal cyanide nitrogen of a neighbouring chain [2.796(5) Å for O(13)···N(2)] (Fig. 5 and Fig. 6) leading to a two-dimensional structure. Graphite-like interactions are observed between the ampy ligands of neighbouring chains, the interplanar separation being 3.43 [ampy···ampy ($1-x$, $-y$, $1-z$)] and 3.41 [ampy···ampy ($2-x$, $-y$, $1-z$)] Å. The values of the intrachain chromium-manganese separation through bridging cyanide are 5.295(1) [Cr(1)···Mn(1)] and 5.365(2) [Mn(1)···Cr(1f); (f) = $1+x$, y, z] Å. Other relevant intrachain metal-metal distances are 7.191(1) [Mn(1)···Mn(1b) and Cr(1)···Cr(1b); (b) = $-1+x$, y, z] and 7.870(1) [Cr(1)···Cr(1g); (g) = $1-x$, $-y$, $-z$] Å. The values of the interchain metal-metal distances observed in compound **3** are 6.151(1) [Cr(1)···Cr(1j); (j) = $2-x$, $1-y$, $1-z$], 7.463(1) [Cr(1)···Cr(1k); (k) = $1-x$, $1-y$, $1-2z$], 8.884(2) [Mn(1)···Cr(1e); (e) = x, $y-1$, z] and 10.566(1) [Mn(1)···Mn(1n); (n) = x, $-1+y$, z] Å.

Each chain in **4** is surrounded by four other chains with two orientations (Fig. 7). Each coordinated water molecule (Table 5) is connected to two crystallisation water molecules through hydrogen bonds [2.819(8) and 2.705(7) Å for O(1)···O(2i) and O(1)···O(3a), respectively; (i) = $-1/2+x$, $1/2-y$, $1/2+z$ and (a) = $-x$, $1-y$, $1-z$]. These crystallisation molecules are themselves hydrogen-bonded to the nitrogen atoms of the two terminal cyanide groups of the chromium centres of neighbouring chains [2.828(8) and 2.990(8) Å for N(2)···O(3j) and N(3)···O(2a), respectively; (j) = $-1/2+x$, $3/2-y$, $1/2+z$] (Fig. 7), leading in this way to a three-dimensional structure. No π–π interactions between the aromatic ligands of adjacent chains are observed in the packing of **4**. The values of the

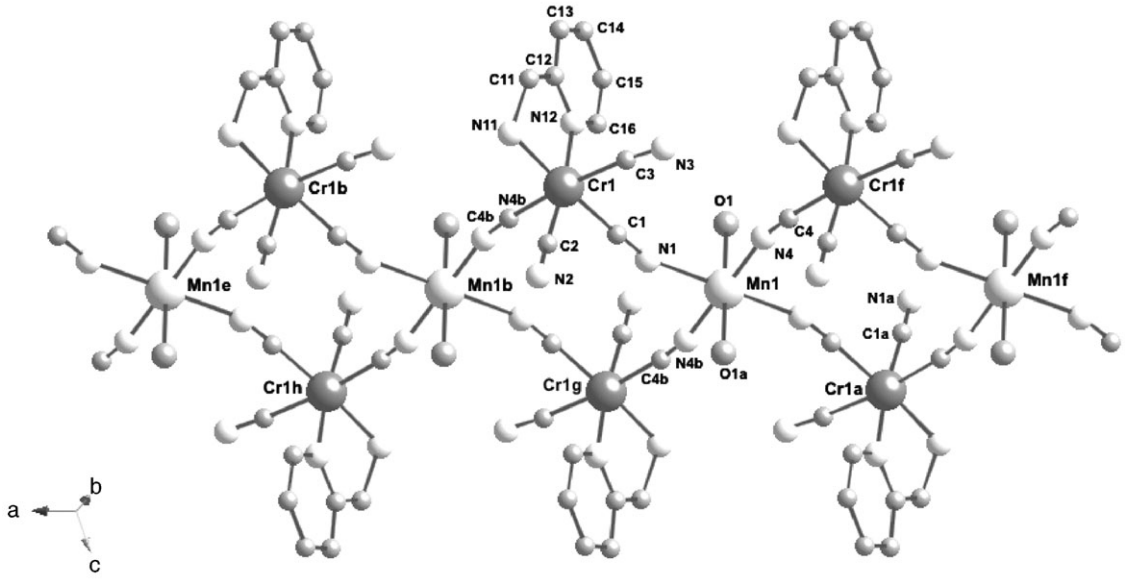

Fig. 3 Perspective view of a fragment of the crossed zigzag chain of **3** running parallel to the *a* axis and including the atom numbering of the asymmetric unit.

intrachain chromium-manganese separation through bridging cyanide are 5.343(1) [Cr(1)···Mn(1)] and 5.288(1) [Mn(1)···Cr(1b); (b) = $-1-x$, $1-y$, $1-z$] Å. Other relevant intrachain metal-metal distances are 7.641(5) [Mn(1)···Mn(1c) and Cr(1)···Cr(1c); (c) = $-1+x$, y, z] and 7.392(2) [Cr(1)···Cr(1b)] Å. The shortest interchain Cr(1)···Cr(1m), Mn(1)···Mn(1l) and Mn(1)···Cr(1k) distances are 8.575(1), 11.462(1) and 7.547(1) Å, respectively [(k) = $-1/2-x$, $-1/2+y$, $3/2-z$; (l) = $-1/2-x$, $-1/2+y$, $1/2-z$; (m) = $-1/2-x$, $-1/2+y$, $3/2-z$)].

The chromium and manganese atoms in **3** and **4** are six-coordinate: two nitrogen atoms from the aromatic ligand and four cyanide carbon atoms around the chromium centre, whereas around the manganese centre two water molecules in *trans* positions plus four cyanide nitrogen atoms build distorted octahedral geometries. The bond distances and angles around the chromium atom in the $[Cr(L)(CN)_4]^-$ unit of **3** and **4** agree with those observed for this unit in **1** and **2**, respectively. The values of the Cr(1)–C–N angle for the bridging cyanides are 172.0(3)°, 178.8(3)° (**3**) or 174.4(5)° and 176.0(5)° (**4**), whereas those of the terminal cyanides are 178.8(5)°, 173.6(3)° (**3**) or 178.0(5)° and 178.5(5)° (**4**). The lengths of the Mn–O_{water} bond are 2.198(3) (**3**) and 2.176(4) (**4**) Å. The Mn–N(cyanide) bond lengths are 2.184(3) and 2.217(3) Å in **3** and 2.190(5) and 2.244(5) Å in **4**. Large departures from strict linearity of the bond angles at the Mn–N–C fragments are observed: 161.3(3)° (**3**) and 161.7(5)° (**4**) for Mn(1)–N(1)–C(1) and 169.0(3)° (**3**) and 159.6(5)° (**4**) for Mn(1)–N(4)–C(4). The C–N bond lengths for terminal and bridging cyanide ligands [1.145(5)–1.138(4) Å (**3**) and 1.137(7)–1.116(8) Å (**4**)] compare well with those observed in **1** and **2**.

The IR spectra of **3** and **4** provide spectral evidence for the occurrence of bridging [2167s (**3**) and 2164m (**4**) cm^{-1}] and terminal [2139w, 2130m (**3**) and 2153w, 2143w (**4**) cm^{-1}] cyanide ligands. The N(12), C(11), C(12), C(13), C(14), C(15) and C(16) atoms of the ampy ligand are coplanar [N(11) and Cr(1) are shifted by 0.50 and 0.07 Å, respectively, from this mean plane].

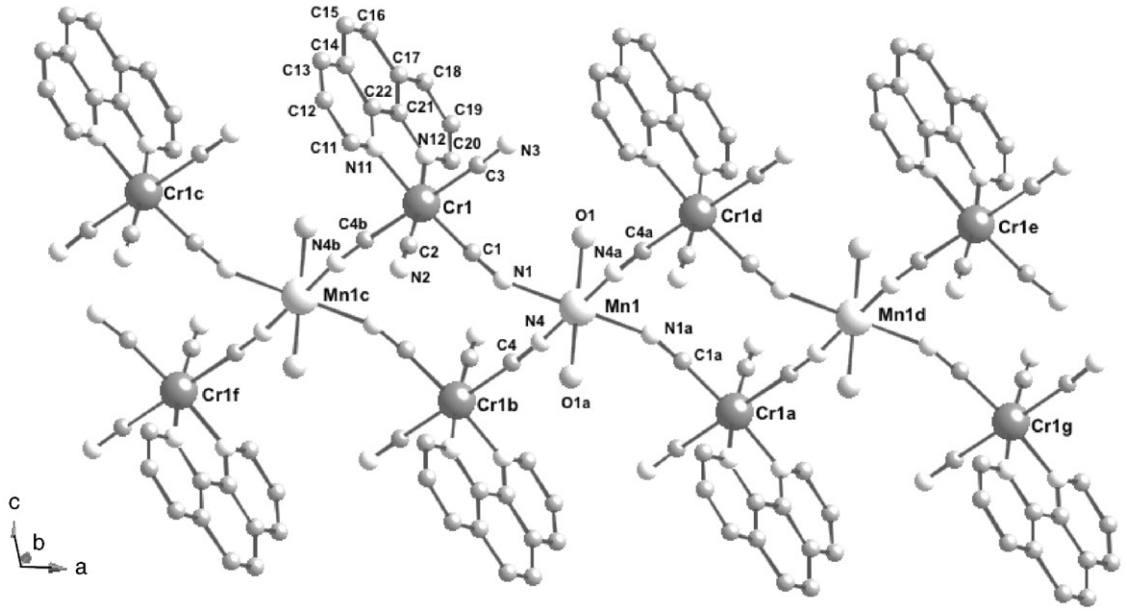

Fig. 4 Perspective view of a fragment of the crossed zigzag chain of **4** running parallel to the *a* axis and showing the atom numbering of the asymmetric unit.

Table 4 Selected bond distances (Å) and angles (°) in complex **3**[ab]

Cr(1)–N(11)	2.071(3)	Cr(1)–N(12)	2.068(2)
Cr(1)–C(1)	2.050(3)	Cr(1)–C(2)	2.045(4)
Cr(1)–C(3)	2.082(3)	Cr(1)–C(4b)	2.061(3)
Mn(1)–N(1)	2.184(3)	Mn(1)–N(4)	2.217(3)
Mn(1)–O(1)	2.198(3)	C(1)–N(1)	1.140(5)
C(2)–N(2)	1.145(5)	C(3)–N(3)	1.138(4)
C(4)–N(4)	1.139(4)		
N(11)–Cr(1)–N(12)	79.30(10)	N(11)–Cr(1)–C(1)	174.68(11)
N(11)–Cr(1)–C(2)	93.14(15)	N(11)–Cr(1)–C(3)	92.69(11)
N(11)–Cr(1)–C(4b)	94.71(11)	N(12)–Cr(1)–C(1)	95.40(12)
N(12)–Cr(1)–C(2)	172.42(14)	N(12)–Cr(1)–C(3)	90.19(10)
N(12)–Cr(1)–C(4b)	89.81(11)	C(1)–Cr(1)–C(2)	92.16(16)
C(1)–Cr(1)–C(3)	86.91(12)	C(1)–Cr(1)–C(4b)	85.60(12)
C(2)–Cr(1)–C(3)	89.63(14)	C(2)–Cr(1)–C(4b)	91.35(15)
C(3)–Cr(1)–C(4b)	172.47(12)	N(1)–Mn(1)–N(4)	87.60(12)
N(1)–Mn(1)–N(4a)	92.40(12)	N(1)–Mn(1)–O(1)	89.57(13)
N(1)–Mn(1)–O(1a)	90.43(13)	N(4)–Mn(1)–O(1)	91.28(12)
N(4a)–Mn(1)–O(1)	88.72(12)	Cr(1)–C(1)–N(1)	178.0(3)
Cr(1)–C(2)–N(2)	178.8(5)	Cr(1)–C(3)–N(3)	173.6(3)
Cr(1)–C(4b)–N(4b)	172.0(3)	Mn(1)–N(1)–C(1)	161.3(3)
Ma(1)–N(4)–C(4)	169.0(3)		

Hydrogen bonds[bc]	A	D	A···D
	O(1)	O(12c)	2.646(7)
	O(1)	O(13d)	2.738(5)
	O(11)	O(12)	2.741(9)
	O(13)	N(2)	2.796(5)

[a] Estimated standard deviations in the last significant digits are given in parentheses. [b] Symmetry code: (a) = $2-x, -y, -z$; (b) = $-1+x, y, z$; (c) = $1+x, -1+y, z$; (d) = $x, -1+y, z$. [c] A = acceptor, D = donor.

Magnetic properties

The magnetic properties of complexes **1** and **2** in the form of the $\chi_M T$ product against T plot [χ_M being the magnetic susceptibility per mol of Cr(III)] are shown in Fig. S5 in the ESI and Fig. 8, respectively. They are very close, as expected, given that they concern mononuclear chromium(III) complexes that are isolated from each other by bulky tetraphenylphosphonium cations. At room temperature, $\chi_M T$ for **2** is 1.86 cm^3 mol^{-1} K (1.84 cm^3 mol^{-1} K for **1**), a value expected for a magnetically isolated spin quartet. It remains constant upon cooling and only decreases slightly at very low temperatures, reaching 1.77 cm^3 mol^{-1} K at 1.9 K (1.70 cm^3 mol^{-1} K for **1**). No susceptibility maximum was observed within the temperature range investigated for **1** and **2**. The slight decrease of $\chi_M T$ at lower temperatures may be attributed to the zero field splitting (D) of the chromium(III) ion, to weak antiferromagnetic intermolecular interactions, or to both factors simultaneously. In agreement with the mononuclear nature of **1** and **2**, their magnetic data have been analysed through the Hamiltonian given by eqn. (1) , in the case of an axial zero field splitting and S = 3/2:[31]

$$\hat{H} = D\,[\hat{S}_z^{\,2} - 1/3S(S+1)] \qquad (1)$$

Least-squares fit of the $\chi_M T$ data of **2** (**1**) through the expression derived from eqn. (1) leads to the following set of parameters: $|D|$ = 0.88 (1.2) cm^{-1}, g = 1.99 (1.98) and $R = 3.5 \times 10^{-6}$ (1.3×10^{-6}). R is the agreement factor defined as $\Sigma_i[(\chi_M T)_{obsd}(i) - (\chi_M T)_{calcd}(i)]^2/\Sigma_i[(\chi_M T)_{obsd}(i)]^2$. The computed curves match well the experimental data over the whole temperature range. The magnetisation data at 2.0 K can be reproduced theoretically with these D and g values (see inset of

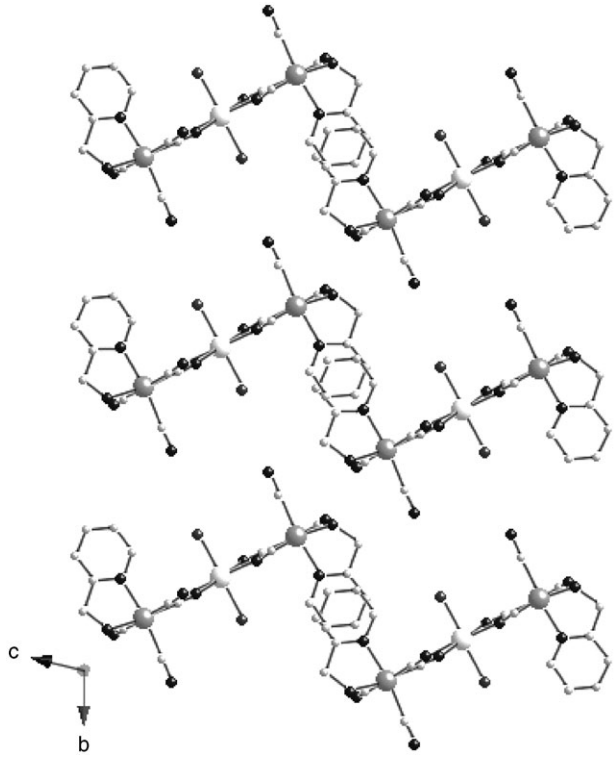

Fig. 5 View of the arrangement of the bimetallic chains of **3** in the *bc* plane showing their unique orientation. Crystallisation water molecules are omitted for the sake of clarity.

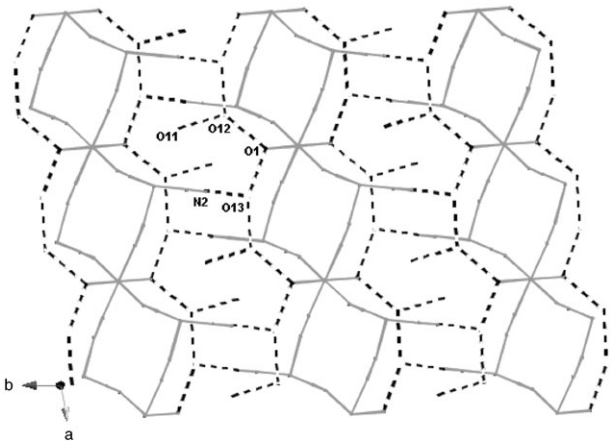

Fig. 6 Schematic representation of the parallel zigzag chains of **3** where only the metal and oxygen atoms and the cyanide bridges (full lines) are included. The hydrogen bonds between the chains are noted as dashed lines.

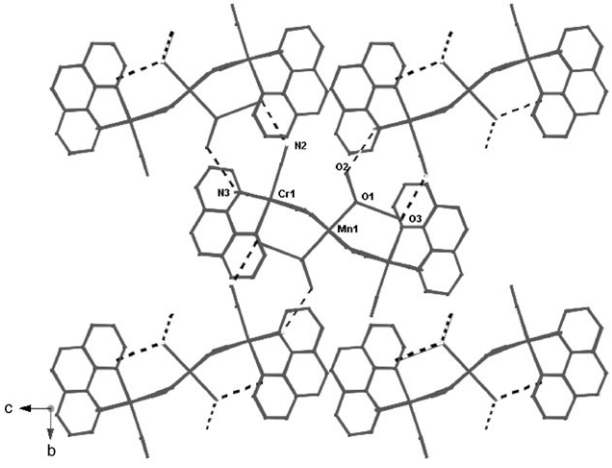

Fig. 7 A projection along the *a* axis showing the two orientations of the chains in **4** together with the hydrogen bonds between them (dashed lines).

Table 5 Selected bond distances (Å) and angles (°) in complex **4**[ab]

Cr(1)–N(11)	2.067(4)	Cr(1)–N(12)	2.069(5)
Cr(1)–C(1)	2.054(6)	Cr(1)–C(2)	2.043(6)
Cr(1)–C(3)	2.071(6)	Cr(1)–C(4b)	2.067(6)
Mn(1)–N(1)	2.244(5)	Mn(1)–N(4)	2.190(5)
Mn(1)–O(1)	2.176(4)	C(1)–N(1)	1.137(7)
C(2)–N(2)	1.133(8)	C(3)–N(3)	1.116(8)
C(4)–N(4)	1.135(7)		
N(11)–Cr(1)–N(12)	79.80(17)	N(11)–Cr(1)–C(1)	174.4(2)
N(11)–Cr(1)–C(2)	93.7(2)	N(11)–Cr(1)–C(3)	87.1(2)
N(11)–Cr(1)–C(4b)	93.84(19)	N(12)–Cr(1)–C(1)	96.6(2)
N(12)–Cr(1)–C(2)	173.2(2)	N(12)–Cr(1)–C(3)	90.4(2)
N(12)–Cr(1)–C(4b)	88.5(2)	C(1)–Cr(1)–C(2)	90.1(2)
C(1)–Cr(1)–C(3)	88.7(2)	C(1)–Cr(1)–C(4b)	90.3(2)
C(2)–Cr(1)–C(3)	91.3(2)	C(2)–Cr(1)–C(4b)	89.9(2)
C(3)–Cr(1)–C(4b)	178.4(2)	N(1)–Mn(1)–N(4)	89.8(2)
N(1)–Mn(1)–N(4a)	90.2(2)	N(1)–Mn(1)–O(1)	86.44(19)
N(1a)–Mn(1)–O(1)	93.56(19)	N(4)–Mn(1)–O(1)	90.27(19)
N(4a)–Mn(1)–O(1)	89.73(19)	Cr(1)–C(1)–N(1)	174.4(5)
Cr(1)–C(2)–N(2)	178.0(5)	Cr(1)–C(3)–N(3)	178.5(5)
Cr(1)–C(4b)–N(4b)	176.0(5)	Mn(1)–N(1)–C(1)	161.7(5)
Mn(1)–N(4)–C(4)	159.6(5)		

Hydrogen bonds[bc]	A	D	A···D
	O(1)	O(2i)	2.819(8)
	O(1)	O(3a)	2.705(7)
	O(3j)	N(2)	2.828(8)
	O(2a)	N(3)	2.990(8)

[a] Estimated standard deviations in the last significant digits are given in parentheses. [b] Symmetry code: (a) = $2-x, -y, -z$; (b) = $-1+x, y, z$. (i) = $-1/2+x, 1/2-y, 1/2+z$; (j) = $-1/2+x, 3/2-y, 1/2+z$. [c] A = acceptor, D = donor.

Fig. 8). So, it is clear that we are dealing with a magnetically isolated spin quartet with a very weak magnetic anisotropy. The large value of the shortest intermolecular chromium-chromium separation [**1**: 6.325(1) and **2**: 8.094(1) Å, see Figures S2 (**1**) and S4 (**2**) in the ESI] accounts for the good fit with D and g as variable parameters.

The magnetic properties of complex **3** in the form of the $\chi_M T$ product against T plot [χ_M being the magnetic susceptibility per mol of $Cr^{III}_2Mn^{II}$ unit] are shown in Fig. 9. $\chi_M T$ at 295 K is 7.0 $cm^3\ mol^{-1}$ K, a value that is clearly below that calculated for two magnetically isolated spin quartets [Cr(III)] and one

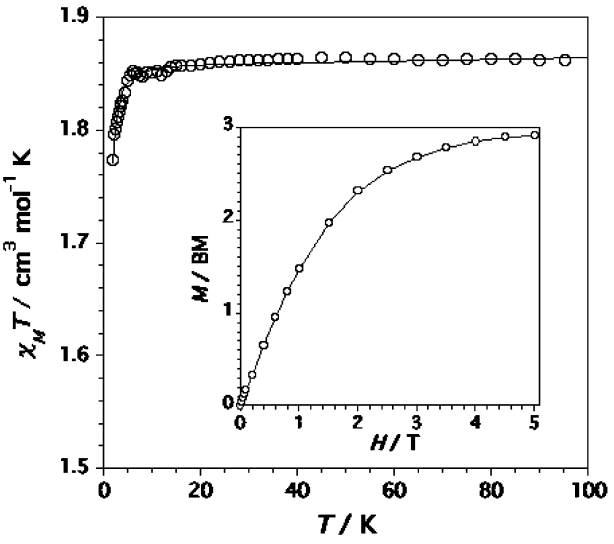

Fig. 8 $\chi_M T$ *versus* T plot for complex **2**: (○) experimental data; (—) best fit through eqn. (1). The inset shows the magnetisation against the applied magnetic field at 2.0 K: (○) experimental data; (—) Brillouin function for a magnetically isolated spin $S = 3/2$ with $g = 1.99$.

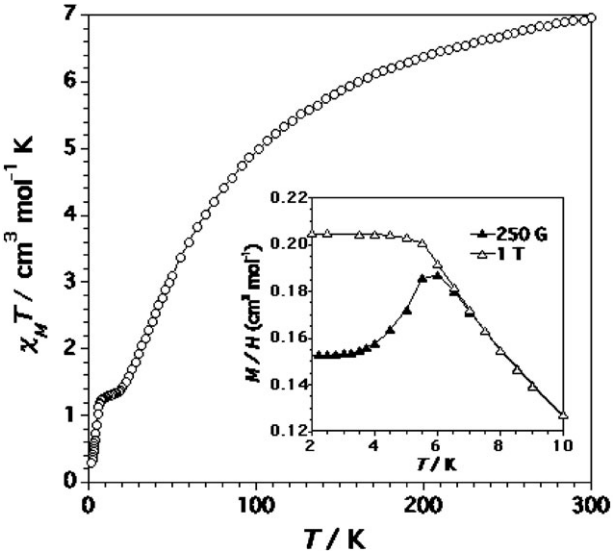

Fig. 9 $\chi_M T$ *versus* T plot for complex **3** under applied magnetic fields of 1 T ($T > 50$ K) and 250 G ($T \leq 50$ K). The inset shows the thermal dependence of the magnetic susceptibility at $T \leq 10$ K and under applied magnetic fields of 250 G (▲) and 1 T (Δ).

spin sextet [Mn(II), 8.13 $cm^3\ mol^{-1}$ K with $g = 2.0$]. This value continuously decreases upon cooling, then tends to a plateau with $\chi_M T = 1.30\ cm^3\ mol^{-1}$ K at $T \leq 15$ K and finally decreases at lower temperatures to reach $\chi_M T = 0.30\ cm^3\ mol^{-1}$ K at 1.9 K. As shown in the inset of Fig. 9, there is a maximum in the susceptibility (M/H) at 6.0 K in the χ_M *versus* T curves measured at low magnetic field ($H < 1$ T), which disappears at higher fields. No signal was observed for the ac magnetic susceptibility measurements of **3** at $T < 15$ K.

The magnetic features of complex **3** can be interpreted as follows: the intrachain antiferromagnetic interaction between chromium(III) and manganese(II) ions through the two single cyanide bridges accounts for the strong decrease of $\chi_M T$ in the high temperature range of Fig. 9; the lack of the expected minimum in the $\chi_M T$ *versus* T plot of the resulting ferrimagnetic chain is due to the interchain antiferromagnetic interactions, which are evidenced by the susceptibility maximum at 6.0 K under low applied magnetic fields. This maximum disappears for $H \geq 1$ T and thus the magnetic behaviour of

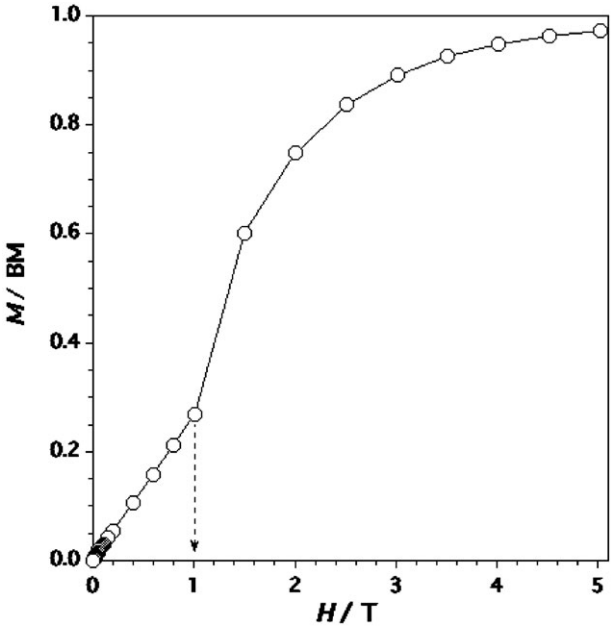

Fig. 10 Magnetisation *versus* H plot of **3** at 2.0 K.

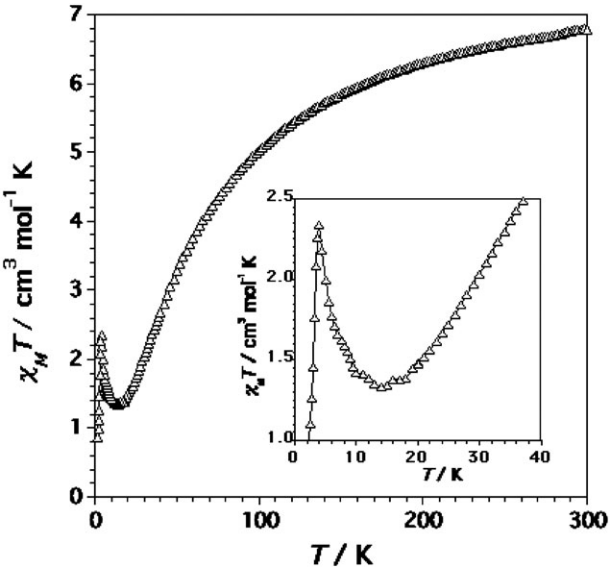

Fig. 11 $\chi_M T$ *versus* T plot for complex **4** under applied magnetic fields of 1 T ($T > 50$ K) and 250 G ($T \leq 50$ K). The inset shows the region of the minimum in $\chi_M T$.

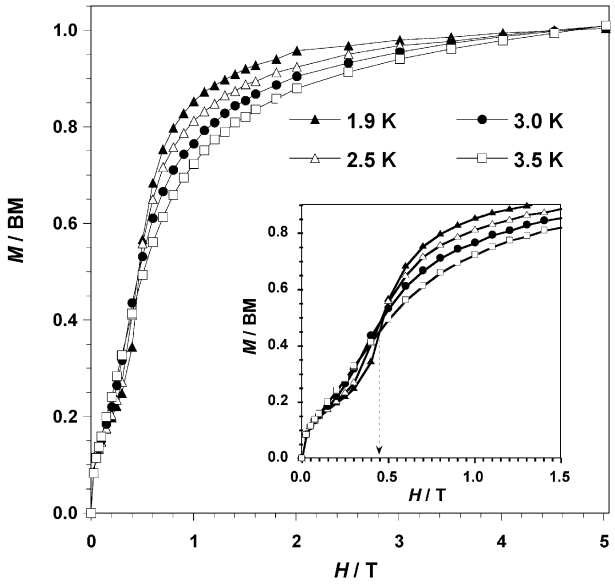

Fig. 13 Isotherms ($1.9 \leq T \leq 3.5$ K) of the magnetisation *versus* H plot for **4**. The inset shows a detail of the low-field domain.

complex **3** is that expected for a metamagnet. This interpretation is supported by the magnetisation plot for the $Cr^{III}_2Mn^{II}$ unit of **3** at 2.0 K (Fig. 10). The quasi-saturation value of the magnetisation at 5 T (the maximum magnetic field in our SQUID) is 0.97 BM. This value is as expected for a low-lying spin doublet with $g = 1.98$ ($S = 2S_{Cr^{III}} - S_{Mn^{II}} = 6/2 - 5/2 = 1/2$). The sigmoidal shape of the M *versus* H plot is the signature of the metamagnetic behaviour of **3**.[32] The value of the critical field, $H_c = 1$ T, allows the estimation of a value for the interchain magnetic interaction of *ca.* 1 cm^{-1}. The evaluation of the intrachain antiferromagnetic interactions in **3** is precluded by the lack of a suitable model to analyse the magnetic data of a 4,2-ribbon-like chain, the local spins being 3/2 (Cr^{III}) and 5/2 (Mn^{II}). Recent works have shown that the magnetic coupling (J) between Cr^{III} and Mn^{II} ions through a single cyanide bridge is antiferromagnetic and the quoted values are -6.2 cm^{-1} for a trinuclear complex of formula $\{[Cr(bipy)(CN)_4]_2Mn(H_2O)_4 \cdot 4H_2O\}$[28] and -7.2 and -10.8 cm^{-1} for a heptanuclear complex of formula $\{Cr[CNMn(tetren)]_6\}_2[Mn(tetren)(H_2O)]_2(ClO_4)_{22}$ with tetren = tetraethylenepentamine.[33]

The magnetic properties of complex **4** in the form of the $\chi_M T$ product against T plot [χ_M being the magnetic susceptibility per mol of $Cr^{III}_2Mn^{II}$ unit] are shown in Fig. 11. The value of $\chi_M T$ at 300 K is 6.80 cm^3 mol^{-1} K. As in **3**, this value is below that calculated for two magnetically isolated spin quartets [Cr(III)] and one spin sextet [Mn(II), 8.13 cm^3 mol^{-1} K with $g = 2.0$]. Upon cooling, $\chi_M T$ strongly decreases and reaches a minimum at 14 K with an $\chi_M T$ of 1.35 cm^3 mol^{-1} K. At lower termperatures, it increases to 2.25 cm^3 mol^{-1} K at 4.0 K before finally decreasing to *ca.* 0.82 cm^3 mol^{-1} K at 1.9 K. A maximum in the susceptibility is observed for **4** at $T = 4$ K (under low magnetic fields), indicating the presence of interchain antiferromagnetic interactions. This maximum disappears for $H \geq 5000$ G (Fig. 12). The magnetisation *versus* H plot at different temperatures (Fig. 13) tends to a saturation value of 1.0 BM at 5 T. This value is as expected for a ground doublet spin state with $g = 2.0$ ($S = 2S_{Cr} - S_{Mn} = 6/2 - 5/2 = 1/2$). The sigmoidal shape of the field-dependent magnetisation below 4 K (see Fig. 13) is the signature of the

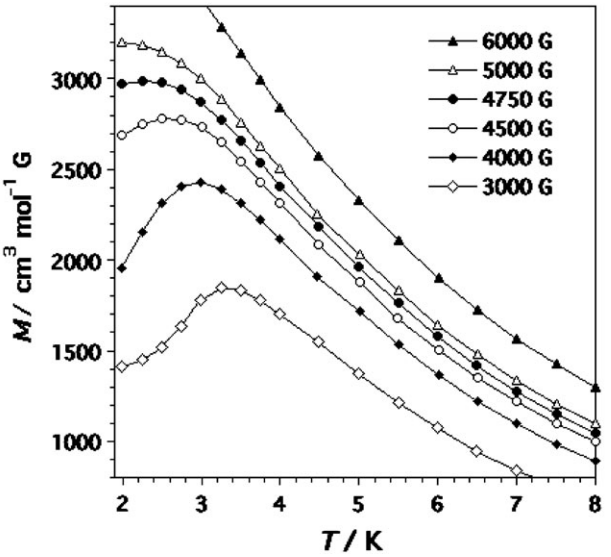

Fig. 12 M *versus* T plot of **4** as a function of the applied magnetic field.

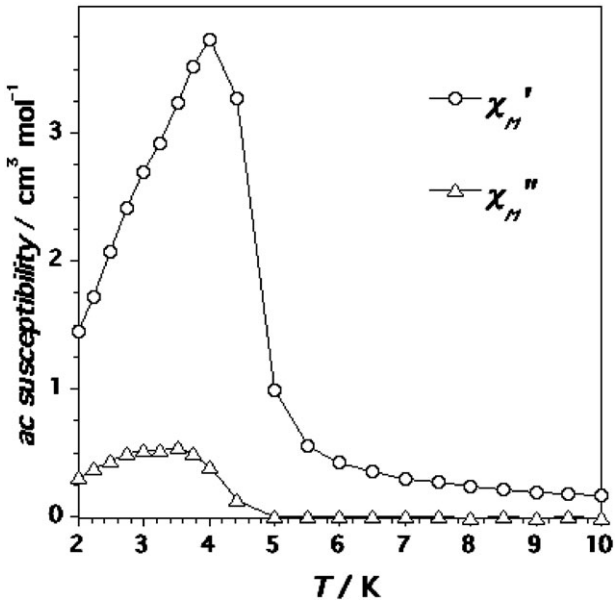

Fig. 14 Thermal dependence of the in-phase and out-of-phase ac susceptibility signals for **4** in the absence of applied external field and under an oscillating magnetic field of ±1 G.

metamagnetic behaviour of **4**. The value of the critical field H_c = 5000 G (the inflexion point in the inset of Fig. 13) allows the estimation of a value for the interchain interaction of *ca.* 0.5 cm^{-1}. Ac measurements of **4** show frequency-independent maxima in the in-phase and out-of-phase components at very low temperatures (Fig. 14). This magnetic ordering can be attributed to a spin-canted structure below 4 K. In the inset of Fig. 13, one can see an incipient saturation of the magnetisation at 0.15 BM and *ca.* 0.1 T. This anomaly in the magnetisation plot is due to the spin canting. Indeed, the magnetisation loop of **4** at 2.0 K exhibits a small hysteresis loop with a weak coercive field of *ca.* 50 G (Figure S6 in the ESI). These magnetic features of **4** can be interpreted on the basis of its molecular structure. The non-compensation between the antiferromagnetically coupled spins of the interacting Cr^{III} and Mn^{II} ions leads to a ferromagnetic chain as in **3** and accounts for the shape of the $\chi_M T$ *versus* T plot (decrease of $\chi_M T$ in the high temperature range with a minimum of $\chi_M T$ at 14 K). The interchain antiferromagnetic interactions account for the maximum of the susceptibility in the low-temperature domain. This maximum disappears when the energy provided by the applied magnetic field is on the order of magnitude of the interchain antiferromagnetic interactions leading to the observed metamagnetism. The value of the critical field for **4** (H_c = 5000 G) is smaller than that of **3** (H_c = 1 T), indicating that the interchain magnetic interactions in **4** are weaker. This is in agreement with the shorter interchain metal-metal separation in **3** [6.151(1) Å in **3** *versus* 8.575(1) Å in **4**]. In contrast to compound **3**, which exhibits a clear antiferromagnetic ordering, compound **4** shows a weak ferromagnetism due to a spin canting. As the centrosymmetric character of the spatial group of **4** (whose structure contains two different orientations of the bimetallic chains *versus* only one in compound **3**) is incompatible with the spin canting, we think that a structural change to a noncentrosymmetric structure has to occur in **4** at very low temperatures.

Conclusions

The use of the stable tetracyanometallate $[CrL(CN)_4]^-$ species [L = ampy (**1**) and phen (**2**)] as complex ligands towards fully hydrated manganese(II) ions provided the new cyanide-bridged 4,2-ribbon-like bimetallic chains $\{[Cr(ampy)(CN)_4]_2Mn(H_2O)_2\}\cdot 6H_2O$ (**3**) and $\{[Cr(phen)(CN)_4]_2Mn(H_2O)_2\}\cdot 4H_2O$ (**4**), which behave as metamagnets with H_c values of 1 T (**3**) and 5000 G (**4**). Magnetic ordering below 4 K is observed for **4** due to a spin canting. The results presented here show that stable tailored precursors such as complexes **1** and **2** are suitable building blocks to access to new molecule-based magnets in a near future.

Acknowledgements

We thank the Ministerio Español de Ciencia y Tecnología (Project BQU-2001-2928), the French CNRS and the European Union (Project QuEMolNa, MRTN-CT-2003-504880) for financial support. One of us (L. Toma) acknowledge the Ministerio Español de Educación, Cultura y Deporte for a predoctoral fellowship.

References

1 K. R. Dunbar and R. A. Heintz, *Prog. Inorg. Chem.*, 1997, **45**, 283, and references therein.
2 M. Verdaguer, A. Bleuzen, V. Marvaud, J. Vaissermann, M. Seuleiman, C. Desplanches, A. Scuiller, C. Train, R. Garde, G. Gelly, C. Lomenech, I. Rosenman, P. Veillet, C. Cartier and F. Villain, *Coord. Chem. Rev.*, 1999, **190–192**, 1023, and references therein.
3 (*a*) D. William, J. Kouvetakis and M. O'Keefe, *Inorg. Chem.*, 1998, **37**, 4617; (*b*) M. P. Shores, L. G. Beauvais and J. R. Long, *J. Am. Chem. Soc.*, 1999, **121**, 775; (*c*) M. P. Shores, L. G. Beauvais and J. R. Long, *Inorg. Chem.*, 1999, **38**, 1648; (*d*) M. V. Bennett, L. G. Beauvais, M. P. Shores and J. R. Long, *J. Am. Chem. Soc.*, 2001, **123**, 8022.
4 (*a*) K. K. Klausmeyer, T. B. Rauchfuss and S. R. Wilson, *Angew. Chem., Int. Ed.*, 1998, **37**, 1694; (*b*) A. M. A. Ibrahim, *Polyhedron*, 1999, **18**, 2111.
5 D. J. Darensbourg and A. L. Phelps, *Inorg. Chim. Acta*, 2004, **357**, 1603, and references therein.
6 (*a*) T. Mallah, S. Thiébault, M. Verdaguer and P. Veillet, *Science*, 1993, **262**, 1554; (*b*) S. Ferlay, T. Mallah, R. Ouahès, P. Veillet and M. Verdaguer, *Nature (London)*, 1995, **378**, 701; (*c*) R. Garde, F. Villain and M. Verdaguer, *J. Am. Chem. Soc.*, 2002, **124**, 10531.
7 (*a*) W. R. Entley and G. S. Girolami, *Science*, 1995, **268**, 397; (*b*) S. M. Holmes and G. S. Girolami, *J. Am. Chem. Soc.*, 1999, **121**, 5593.
8 Ø. Hatlevik, W. E. Buschmann, J. Zhang, J. L. Manson and J. S. Miller, *Adv. Mater.*, 1999, **11**, 914.
9 (*a*) O. Sato, T. Iyoda, A. Fujishima and K. Hashimoto, *Science*, 1996, **271**, 49; (*b*) O. Sato, S. Hayami, Y. Einaga and Z. Z. Gu, *Bull. Chem. Soc. Jpn.*, 2003, **76**, 443.
10 (*a*) O. Sato, T. Iyoda, A. Fujishima and K. Hashimoto, *Science*, 1996, **272**, 704; (*b*) Z. Z. Gu, O. Sato, T. Iyoda, K. Hashimoto and A. Fujishima, *Chem. Mater.*, 1997, **9**, 1082; (*c*) A. Bleuzen, C. Lomenech, V. Escax, F. Villain, F. Varret, C. Cartier dit Moulin and M. Verdaguer, *J. Am. Chem. Soc.*, 2000, **122**, 6648; (*d*) C. Cartier dit Moulin, F. Villain, A. Bleuzen, M. A. Arrio, P. Sainctavit, C. Lomenech, V. Escax, F. Baudelet, E. Dartyge, J. J. Gallet and M. Verdaguer, *J. Am. Chem. Soc.*, 2000, **122**, 6653; (*e*) D. A. Pejakovic, J. Manson, J. S. Miller and A. Epstein, *J. Phys. Rev. Lett.*, 2000, **85**, 1994; (*f*) V. Escax, A. Bleuzen, C. Cartuer dit Moulin, F. Villain, A. Goujon, F. Varret and M. Verdaguer, *J. Am. Chem. Soc.*, 2001, **123**, 12536; (*g*) G. Champion, V. Escax, C. Cartier dit Moulin, A. Bleuzen, F. Villain, F. Baudelet, E. Dartyge and M. Verdaguer, *J. Am. Chem. Soc.*, 2001, **123**, 12544; (*h*) R. Garde, F. Villain and M. Verdaguer, *J. Am. Chem. Soc.*, 2002, **124**, 10531.
11 (*a*) M. Mizuno, S. Ohkoshi and K. Hashimoto, *Adv. Mater.*, 2000, **12**, 1855; (*b*) S. Ohkoshi, M. Mizuno, G. Hung and K. Hashimoto, *J. Phys. Chem. B*, 2000, **104**, 8365.
12 (*a*) J. L. Heinrich, P. A. Berseth and J. R. Long, *Chem. Commun.*, 1998, 1231; (*b*) P. A. Berseth, J. J. Sokol, M. P. Shores, J. L. Heinrich and J. R. Long, *J. Am. Chem. Soc.*, 2000, **122**, 8655; (*c*) J. J. Sokol, M. P. Shores and J. R. Long, *Angew. Chem., Int. Ed.*, 2001, **40**, 17; (*d*) M. P. Shores, J. J. Sokol and J. R. Long, *J. Am. Chem. Soc.*, 2002, **124**, 2279; (*e*) J. J. Sokol, M. P. Shores and J. R. Long, *Inorg. Chem.*, 2002, **41**, 3052; (*f*) J. J. Sokol, A. G. Hee and J. R. Long, *J. Am. Chem. Soc.*, 2002, **124**, 7656; (*g*) J. Y. Yang, M. P. Shores, J. J. Sokol and J. R. Long, *Inorg. Chem.*, 2003, **42**, 1403.
13 (*a*) K. K. Klausmeyer, T. B. Rauchfuss and S. R. Wilson, *Angew. Chem., Int. Ed.*, 1998, **37**, 1694; (*b*) K. R. Klausmeyer, S. R. Wilson and T. B. Rauchfuss, *J. Am. Chem. Soc.*, 1999, **121**, 2705; (*c*) S. M. Contakes, K. K. Klausmeyer and T. B. Rauchfuss, *Inorg. Chem.*, 2000, **39**, 2069.
14 (*a*) R. Lescouëzec, F. Lloret, M. Julve, J. Vaissermann, M. Verdaguer, R. Llusar and S. Uriel, *Inorg. Chem.*, 2001, **40**, 2065; (*b*) R. Lescouëzec, F. Lloret, M. Julve, J. Vaissermann and M. Verdaguer, *Inorg. Chem.*, 2002, **41**, 818; (*c*) L. M. Toma, R. Lescouëzec, L. D. Toma, F. Lloret, M. Julve, J. Vaissermann and M. Andruh, *J. Chem. Soc., Dalton Trans.*, 2002, 3171; (*d*) R. Lescouëzec, J. Vaissermann, F. Lloret, M. Julve and M. Verdaguer, *Inorg. Chem.*, 2002, **41**, 5943; (*e*) R. Lescouëzec, J. Vaissermann, C. Ruiz-Pérez, F. Lloret, R. Carrasco, M. Julve, M. Verdaguer, Y. Dromzee and D. Gatteschi, *Angew. Chem., Int. Ed.*, 2003, **42**, 1430; (*f*) L. M. Toma, R. Lescouëzec, F. Lloret, M. Julve, J. Vaissermann and M. Verdaguer, *Chem. Commun.*, 2003, 1850; (*g*) R. Lescouëzec, J. Vaissermann, L. M. Toma, R. Carrasco, F. Lloret and M. Julve, *Inorg. Chem.*, 2004, **43**, 2234.
15 (*a*) W. F. Yeung, W. L. Man, W. T. Wong, T. C. Lau and S. Gao, *Angew. Chem., Int. Ed.*, 2001, **40**, 3031; (*b*) S. Wang, J. L. Zuo, S. Gao, Y. Song, H. C. Zhou, Y. Z. Zhang and X. Z. You, *J. Am. Chem. Soc.*, 2004, **126**, 8900.
16 (*a*) H. Oshio, O. Tamada, H. Onodera, T. Ito, T. Ikoma and S. Tero-Kubota, *Inorg. Chem.*, 1999, **38**, 5686; (*b*) H. Oshio, H. Onodera, O. Tamada, H. Mizutani, T. Hikichi and T. Ito, *Chem.-Eur. J.*, 2000, **6**, 2523; (*c*) H. Oshio, M. Yamamoto and T. Ito, *Inorg. Chem.*, 2002, **41**, 5817.
17 Z. N. Chen, R. Appelt and H. Vahrenkamp, *Inorg. Chim. Acta*, 2000, **309**, 65.
18 J. Kim, S. Han, I. K. Cho, K. Y. Choi, M. Hen, S. Yoon and B. J. Suh, *Polyhedron*, 2004, **23**, 1333.

19 J. Cernák, M. Horendác, I. Potocnák, J. Chomic, A. Horendákova, J. Skorsepa and A. Feher, *Coord. Chem. Rev.*, 2002, **224** 51.
20 (*a*) A. Caneschi, D. Gatteschi, N. Lalioti, C. Sangregorio, R. Sessoli, G. Venturi, A. Vindigni, A. Rettori, M. G. Pini and M. A. Novak, *Angew. Chem., Int. Ed.*, 2001, **40**, 1760; (*b*) A. Caneschi, D. Gatteschi, N. Lalioti, R. Sessoli, L. Sorace, V. Tangoulis and A. Vindigni, *Chem.-Eur. J.*, 2002, **8**, 286; (*c*) R. Clérac, H. Miyasaka, M. Yamashita and C. Coulon, *J. Am. Chem. Soc.*, 2002, **124**, 12837; (*d*) H. Miyasaka, R. Clérac, K. Mizushima, K. Sugiura, M. Yamashita, W. Wernsdorfer and C. Coulon, *Inorg. Chem.*, 2003, **42**, 8203; (*e*) T. F. Liu, D. Fu, S. Gao, Y. Z. Zhang, H. L. Sun, G. Su and Y. J. Liu, *J. Am. Chem. Soc.*, 2003, **125**, 13976; (*f*) S. Wang, J. L. Zuo, S. Gao, Y. Song, H. C. Zhou, Y. Z. Zhang and X. Z. You, *J. Am. Chem. Soc.*, 2004, **126**, 8900.
21 J. C. Revee, *J. Chem. Educ.*, 1985, **62**, 44.
22 A. Earnshaw, *Introduction to Magnetochemistry*, Academic Press, London, 1968.
23 N. Walker and D. Stuart, *Acta Crystallogr., Sect. A*, 1983, **39**, 156.
24 G. M. Sheldrick, *SHELXL-86, A Program for Crystal Structure Solution*, University of Göttingen, Germany, 1986.
25 D. J. Watkin, R. I. Cooper, J. R. Carruthers and P. W. Betteridge, *J. Appl. Crystallogr.*, 2003, **36**, 1487.
26 M. Nardelli, *J. Appl. Crystallogr.*, 1995, **28**, 659.
27 *CRYSTALMAKER 4.2.1*, CrystalMaker Software, Bicester, Oxfordshire, UK, 2001.
28 L. Toma, R. Lescouëzec, J. Vaissermann, F. S. Delgado, C. Ruiz-Pérez, R. Carrasco, J. Cano, F. Lloret and M. Julve, *Chem.-Eur. J.*, 2004, **10**, 6130.
29 I. Dance and M. Scudder, *Chem. Eur. J.*, 1996, **2**, 481.
30 S. Nishigaki, H. Yoshioka and K. Nakaisu, *Acta Crystallogr., Sect. B*, 1978, **34**, 875.
31 C. J. O'Connor, *Prog. Inorg. Chem.*, 1986, **29**, 203.
32 F. Lloret, R. Ruiz, M. Julve, J. Faus, Y. Journaux, I. Castro and M. Verdaguer, *Chem. Mater.*, 1992, **4**, 1150.
33 V. Marvaud, C. Decroix, A. Scuiller, C. Guyard-Duhayon, J. Vaissermann, F. Gonnet and M. Verdaguer, *Chem.-Eur. J.*, 2003, **9**, 1678.